AIAA JOURNAL
Vol. 47, No. 9, September 2009

Technical Notes

Identification of Structural Systems Using an Iterative, Improved Method for System Reduction

Maenghyo Cho* and Sungmin Baek†
Seoul National University, Seoul 151-742, Republic of Korea
Hyungi Kim‡
Korea Aerospace Research Institute, Deajeon 305-333, Republic of Korea
and
Ki-Ook Kim§
Inha University, Incheon 402-751, Republic of Korea

DOI: 10.2514/1.41032

Nomenclature

$\mathbf{K}$	=	stiffness matrix of baseline system
$\mathbf{K}'$	=	stiffness matrix of perturbed system
$\mathbf{K}_e$	=	element stiffness matrix
$\mathbf{M}$	=	mass matrix of baseline system
$\mathbf{M}'$	=	mass matrix of perturbed system
$\mathbf{M}_e$	=	element mass matrix
$\mathbf{R}$	=	vector of residual
$\boldsymbol{\alpha}$	=	input variable of residuals
$\Delta\mathbf{K}$	=	perturbation of stiffness matrix
$\Delta\mathbf{M}$	=	perturbation of mass matrix
$\boldsymbol{\lambda}$	=	eigenvalue of baseline system
$\boldsymbol{\lambda}'$	=	eigenvalue of perturbed system
$\boldsymbol{\varphi}$	=	eigenvector of baseline system
$\boldsymbol{\varphi}'$	=	eigenvector of perturbed system

I. Introduction

EVER-INCREASING capabilities of digital computers have enabled the finite element method (FEM) to serve as a practical tool for the analysis and synthesis of large and complex structures. In practice, however, the automated application of FEM to inverse problems has been limited by the numerous difficulties in mathematical formulation and computational resources. In usual modal methods, the variations of dynamic characteristics, such as natural frequencies and mode shapes, are related to structural modifications.

Several methodologies [1] have been widely used for the identification of structural systems. In the present study, the inverse perturbation method (IPM) [2,3], coupled with improved system reduction, is considered for accelerating solution convergence. Through the condensation, the secondary (slave) degrees of freedom (SDOFs) are eliminated from the problem formulation, whereas the primary (master) degrees of freedom (PDOFs) are included in the system equations. In general, the errors in transformation that are associated with system reduction can be alleviated through the use of various schemes [4–7].

In inverse problems, minor errors in transformation can impair the inverse iterations and convergent solutions cannot be realized. In the neighborhood of a specific eigenvalue, the dynamic stiffness matrix approach [8] exhibits better convergence if the computational efficiency is improved through methods for system reduction. For accelerating of solution convergence, the iterated improved reduced system (IIRS) technique [6] is used.

The specified DOFs are directly related to the placement of the sensor in the vibration test. Hence, a small number of the specified DOFs are defined for the primary set. The solution accuracy and convergence of the reduced system depend upon the proper selection of the PDOFs. The sequential elimination method (SEM) [9] is known to be one of the most reliable selection methods. The major difficulty of the SEM is that the elimination procedure requires considerable computational time. To overcome the disadvantage of SEM, the two-level condensation scheme (TLCS) was proposed by Cho and Kim [10–12]. The TLCS does not require much more computational time than SEM because of the estimation of the energy at the element level [11]. Moreover, the TLCS was combined with a substructuring method [13] for efficiency in the solution of eigenvalue problems.

In this Note for inverse problems, we propose an IIRS technique and that results in a dramatic reduction of the number of DOFs and the required computer resources. The efficient TLCS is employed for the selection of the sensor positions. Numerical examples illustrate that the proposed method can eliminate 80–90% of the computing time that is required in a full-system approach without reduction.

II. Iterative Inverse Perturbation Method (IIPM)

In the finite element analysis, the governing equation for undamped free vibration is presented as

$$\mathbf{K}\,\boldsymbol{\varphi} - \boldsymbol{\lambda}\mathbf{M}\boldsymbol{\varphi} = \mathbf{0} \tag{1}$$

Modifications of the baseline structure produce a perturbed system,

$$\mathbf{K}'\boldsymbol{\varphi}' - \boldsymbol{\lambda}'\mathbf{M}'\boldsymbol{\varphi}' = \mathbf{0} \tag{2}$$

which can be expressed in terms of perturbations:

$$(\mathbf{K} + \Delta\mathbf{K})(\boldsymbol{\varphi} + \Delta\boldsymbol{\varphi}) - (\boldsymbol{\lambda} + \Delta\boldsymbol{\lambda})(\mathbf{M} + \Delta\mathbf{M})(\boldsymbol{\varphi} + \Delta\boldsymbol{\varphi}) = \mathbf{0} \tag{3}$$

To satisfy the new dynamic equilibrium of the perturbed system, the residuals, which are defined in Eq. (4), should be zero because the force equilibrium equation (2) is the necessary and sufficient condition for satisfying the equilibrium of the perturbed system:

$$\mathbf{R} \equiv \mathbf{K}'\boldsymbol{\varphi}' - \boldsymbol{\lambda}'\mathbf{M}'\boldsymbol{\varphi}' = \underbrace{(\mathbf{K} - \boldsymbol{\lambda}'\mathbf{M})\boldsymbol{\varphi}'}_{\text{known}} + \underbrace{(\Delta\mathbf{K} - \boldsymbol{\lambda}'\Delta\mathbf{M})\boldsymbol{\varphi}'}_{\text{unknown}} \tag{4}$$

The structural changes $\Delta\mathbf{K}$ and $\Delta\mathbf{M}$ are determined so that the residuals given in Eq. (4) may become zeros. In this state, the responses of the perturbed system, such as $\boldsymbol{\varphi}'$ and $\boldsymbol{\lambda}'$, are regarded as given values. As shown next, the structural changes are exactly expressed as functions of structural parameters, α_e.

In general, overall responses of the perturbed system $\boldsymbol{\varphi}'$ cannot be defined in the inverse problem because we can detect the responses of

Presented as Paper 2301 at the 48th AIAA/ASME/ASCE/AHS/ASC Structures, Structural Dynamics, and Materials Conference, Honolulu, Hawaii, 23–26 April 2007; received 16 September 2008; revision received 14 February 2009; accepted for publication 16 April 2009.

*Professor, School of Mechanical and Aerospace Engineering; mhcho@snu.ac.kr. Member AIAA.

†Graduate Student, School of Mechanical and Aerospace Engineering; thomas81@snu.ac.kr. Student Member AIAA.

‡Senior Research Engineer, Aeronautic Program Office; shotgun1@kari.re.kr (Corresponding Author).

§Professor, Department of Aerospace Engineering; kokim@inha.ac.kr. Member AIAA.

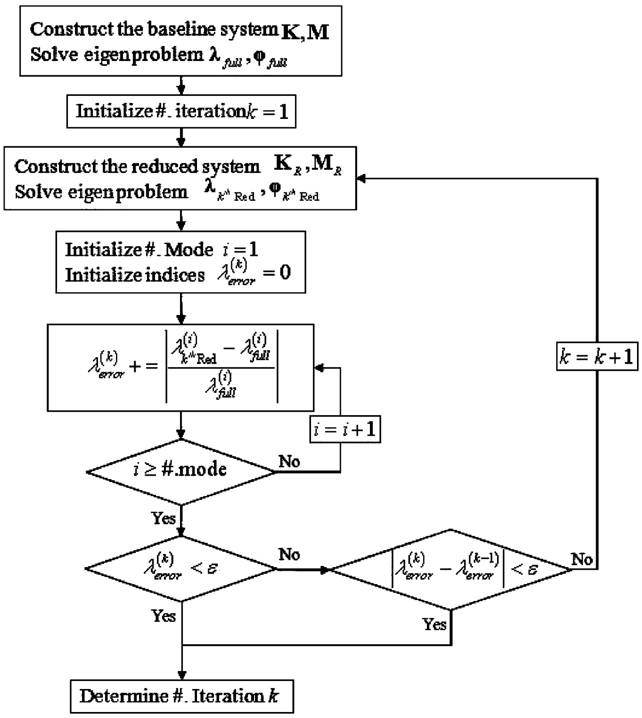

Fig. 1 Schematic for the determination of the number of iterations.

only a limited number of DOFs. The proper selection of the primary set has a significant effect on the convergence of the inverse solution. In this study, the TLCS combined with the substructuring scheme [14] is used to prevent disadvantages of the single-domain approach, such as what the PDOFs might be localized which results in excessive emphasis on lower modes or the loss of important modes.

The unspecified DOFs which have an influence on the solution space can be eliminated in the formulation of residual vectors through the implementation of the transformation matrix of system

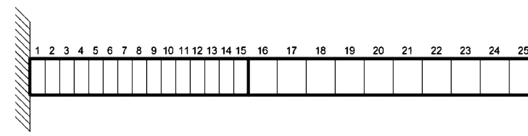

$b = 40mm,\ h = 40mm, L = 3.5m,\ E = 6.9\times10^4\,MPa,\ \nu = 0.33,\ \rho = 2.7\times10^{-9}\,Ns^2/mm^4$

a) Configuration of the cantilever

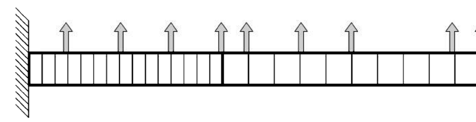

b) Result on the selection of PDOFs using SEM

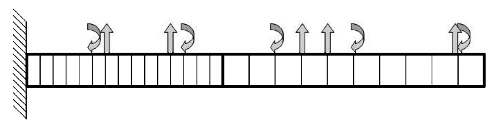

c) Result on the selection of PDOFs using TLCS

Fig. 2 Configuration of the cantilever and results on the selection of PDOFs in the example of the cantilever bending beam.

reduction, $\mathbf{t}(\boldsymbol{\alpha})$. Hence, all the responses of the perturbed system are expressed in terms of the specified responses, $\boldsymbol{\varphi}'_p$:

$$\boldsymbol{\varphi}' = \begin{Bmatrix} \boldsymbol{\varphi}'_p \\ \boldsymbol{\varphi}'_s \end{Bmatrix} = \begin{bmatrix} \mathbf{I} \\ \mathbf{t}(\boldsymbol{\alpha}) \end{bmatrix} \boldsymbol{\varphi}'_p = \mathbf{T}(\boldsymbol{\alpha})\boldsymbol{\varphi}'_p \tag{5}$$

The residual vector (4) is formulated as a simple form in Eq. (6):

$$\mathbf{R}(\boldsymbol{\alpha}) = (\mathbf{K} - \boldsymbol{\lambda}'\mathbf{M})\boldsymbol{\varphi}' + (\Delta\mathbf{K} - \boldsymbol{\lambda}'\Delta\mathbf{M})\boldsymbol{\varphi}'$$
$$\cong \left(\mathbf{K} - \boldsymbol{\lambda}'\mathbf{M} + \sum_{e=1}^{NS} ([S^k(\alpha_e) - \boldsymbol{\lambda}' S^m(\alpha_e)]) \right) \begin{bmatrix} \mathbf{I} \\ \mathbf{t}(\boldsymbol{\alpha}) \end{bmatrix} \boldsymbol{\varphi}'_p \tag{6}$$

We follow the physical approach to determine the weighting matrix in Eq. (7) because the calculation of the gradient of the vector of residuals which was used in the mathematical approach is

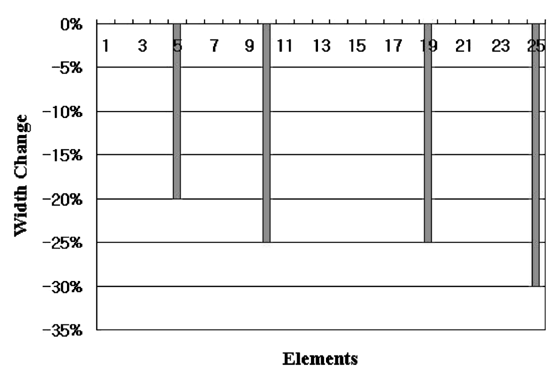

a) Element modification of the perturbed system

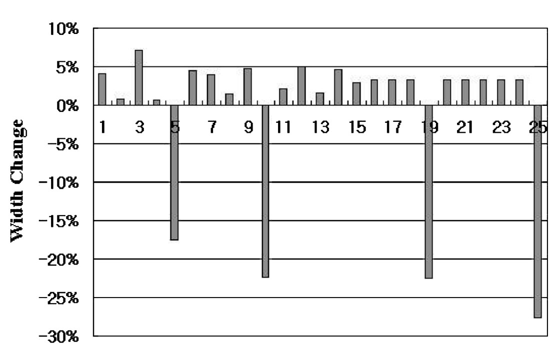

b) Inverse solution using TSEM

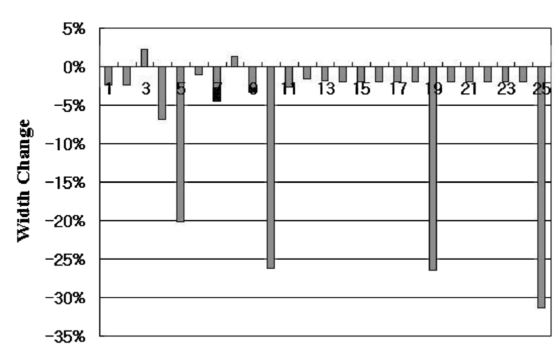

c) Inverse solution using TLCS

Fig. 3 Element modifications of the perturbed system and inverse solution for the example of the cantilever beam (IIPM).

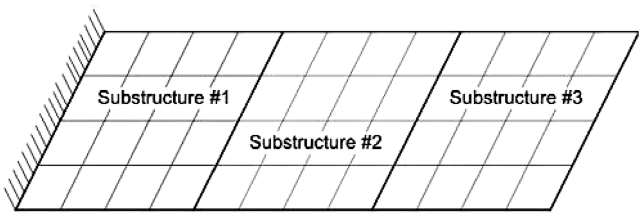

$E = 210GPa, v = 0.33, t = 0.5m, \rho = 7800Kg/m^3$

a) Configuration for the example

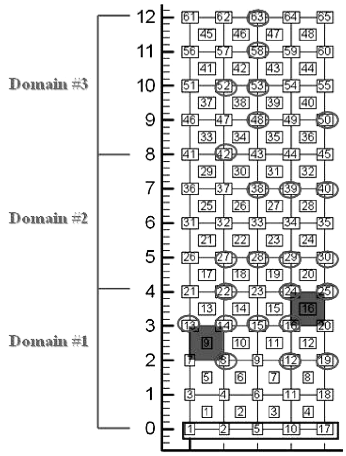

b) Results on the selection of PDOFs

Fig. 4 Configuration of the cantilever and results on the selection of PDOFs in the example of the cantilever plate.

expensive to compute the weighting matrix at each step. The weighting can be approximated as a diagonal matrix by using a new mode shape $\boldsymbol{\varphi}'_j$ as given by

$$W_{ii} = (\phi'_{ij})^2 \tag{7}$$

where the subscript i represents the components of each DOF that consists of a mode vector. The objective function is to minimize the norm of the residuals, as shown in expression (8),

$$\min(\mathbf{R}(\boldsymbol{\alpha})^T \cdot \mathbf{W} \cdot \mathbf{R}(\boldsymbol{\alpha})) \tag{8}$$

Through the weighting matrix, the minimization of the residual force is transformed to the problem of the minimization of the residual energy error at each DOF.

III. Transformation of Degrees of Freedom

Equation (5) represents the transformation from the entire set of DOFs to the specified DOFs. The reliability of the transformation matrix is an essential issue in IIPM because errors in the transformation matrix are magnified in the solution space. The convergence and solution accuracy of IIPM are decisively determined by the accuracy of the transformation matrix $\mathbf{t}(\boldsymbol{\alpha})$. In this section, we outline the IIRS technique, which is the key factor of obtaining an accurate transformation matrix.

The governing equation for undamped, free vibration in Eq. (1) is decomposed into primary and secondary sets of DOFs and rewritten into a decomposed form that constitutes the PDOFs and SDOFs:

$$\begin{bmatrix} \mathbf{K}_{pp} & \mathbf{K}_{ps} \\ \mathbf{K}_{ps}^T & \mathbf{K}_{ss} \end{bmatrix} \begin{Bmatrix} \boldsymbol{\varphi}_p \\ \boldsymbol{\varphi}_s \end{Bmatrix} - \lambda \begin{bmatrix} \mathbf{M}_{pp} & \mathbf{M}_{ps} \\ \mathbf{M}_{ps}^T & \mathbf{M}_{ss} \end{bmatrix} \begin{Bmatrix} \boldsymbol{\varphi}_p \\ \boldsymbol{\varphi}_s \end{Bmatrix} = \begin{Bmatrix} \mathbf{0} \\ \mathbf{0} \end{Bmatrix} \tag{9}$$

The second row of Eq. (9) can be expressed in the following form:

$$\boldsymbol{\varphi}_s = -\mathbf{K}_{ss}^{-1}\mathbf{K}_{ps}^T\boldsymbol{\varphi}_p + \mathbf{K}_{ss}^{-1}(\mathbf{M}_{ps}^T\boldsymbol{\varphi}_p + \mathbf{M}_{ss}\boldsymbol{\varphi}_s)\boldsymbol{\lambda} \tag{10}$$

The transformation matrix between the PDOFs and the SDOFs can be obtained through substituting $\boldsymbol{\varphi}_s = \mathbf{t} \cdot \boldsymbol{\varphi}_p$ into Eq. (10), as shown in Eq. (11):

$$\mathbf{t} = -\mathbf{K}_{ss}^{-1}\mathbf{K}_{ps}^T + \mathbf{K}_{ss}^{-1}(\mathbf{M}_{ps}^T + \mathbf{M}_{ss}\mathbf{t})\boldsymbol{\lambda} \tag{11}$$

Through the transformation matrix, the reduced system can be expressed as shown in Eq. (12):

$$\mathbf{K}_R\boldsymbol{\varphi}_p - \boldsymbol{\lambda}_R\mathbf{M}_R\boldsymbol{\varphi}_p = \mathbf{0} \tag{12}$$

$$\begin{aligned} \mathbf{K}_R &= \mathbf{T}^T\mathbf{K}\mathbf{T} = \mathbf{K}_{pp} + \mathbf{t}^T\mathbf{K}_{ps}^T + \mathbf{K}_{ps}\mathbf{t} + \mathbf{t}^T\mathbf{K}_{ss}\mathbf{t} \\ \mathbf{M}_R &= \mathbf{T}^T\mathbf{M}\mathbf{T} = \mathbf{M}_{pp} + \mathbf{t}^T\mathbf{M}_{ps}^T + \mathbf{M}_{ps}\mathbf{t} + \mathbf{t}^T\mathbf{M}_{ss}\mathbf{t} \end{aligned} \tag{13}$$

The eigenvalue term is approximated from the reduced eigenproblem given in Eq. (12). Substituting $\lambda = \mathbf{M}_R^{-1}\mathbf{K}_R$ into Eq. (11), the transformation matrix evaluated is shown in Eq. (14):

$$\mathbf{t} = -\mathbf{K}_{ss}^{-1}\mathbf{K}_{ps}^T + \mathbf{K}_{ss}^{-1}(\mathbf{M}_{ps}^T + \mathbf{M}_{ss}\mathbf{t})\mathbf{M}_R^{-1}\mathbf{K}_R \tag{14}$$

Table 1 Solution accuracy for eigenvalues in the example of the cantilever flexural bending beam

				Inverse solution					
				Dynamic stiffness matrix [8]		Iterative inverse perturbation method (present)			
Mode	Baseline system	Perturbed system		TSEM		TSEM		TLCS	
1	280.7071	293.395	+4.52%	393.303	+4.49%	293.37	+4.51%	293.522	+4.57%
2	11,024.533	11,494.67	+4.26%	11,494.0	+4.26%	11,493.81	+4.26%	11,495.67	+4.27%
3	86,436.252	90,221.94	+4.38%	90,247.3	+4.41%	90,218.98	+4.41%	90,224.64	+4.38%
4	331,953.33	347,175.39	+4.59%	347,267.0	+4.61%	347,177.14	+4.61%	347,172.64	+4.58%
5	907,278.99	39,674.05	+3.57%	939,922.0	+3.60%	39,673.00	+3.60%	939,676.86	+3.57%

Table 2 Solution accuracy for eigenvalues in the example of the cantilever bending beam

				Inverse solution			
Mode	Baseline system	Perturbed system		Inverse perturbation method [4]		Iterative inverse perturbation method (present)	
1	347.8772	341.0181	−1.972%	341.0242	−1.970%	341.0181	−1.972%
2	12,176.01	11,969.81	−1.693%	11,970.6221	−1.687%	11,969.8146	−1.693%
3	13,493.0	13,456.57	−0.270%	13,456.4866	−0.271%	13,456.5731	−0.270%
4	18,489.92	17,881.76	−3.288%	17,883.5309	−3.280%	17,881.979	−3.288%
5	105,274.3	103,983.4	−1.226%	103,977.7843	−1.232%	103,983.4328	−1.226%

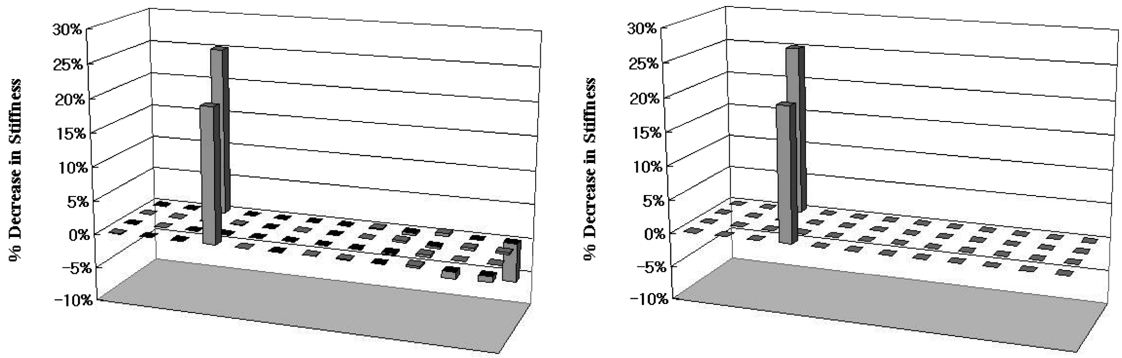

a) IPM with seven lowest modes **b) IIPM with two lowest modes**

Fig. 5 Inverse solutions for the example of the cantilever plate.

Since $\mathbf{t}$ in Eq. (14) is implicit and cannot be directly solved, the iterative scheme is applied as follows:

$$\mathbf{t}^{(k)} = -\mathbf{K}_{ss}^{-1}\mathbf{K}_{ps}^{T} + \mathbf{K}_{ss}^{-1}(\mathbf{M}_{ps}^{T} + \mathbf{M}_{ss}\mathbf{t}^{(k-1)})(\mathbf{M}_{R}^{(k-1)})^{-1}\mathbf{K}_{R}^{(k-1)} \tag{15}$$

$$\begin{aligned}\mathbf{K}_{R}^{(k)} &= (\mathbf{T}^{(k)})^{T}\mathbf{K}\mathbf{T}^{(k)} = \mathbf{K}_{pp} + (\mathbf{t}^{(k)})^{T}\mathbf{K}_{ps}^{T} + \mathbf{K}_{ps}\mathbf{t}^{(k)} \\ &\quad + (\mathbf{t}^{(k)})^{T}\mathbf{K}_{ss}\mathbf{t}^{(k)} \\ \mathbf{M}_{R}^{(k)} &= (\mathbf{T}^{(k)})^{T}\mathbf{M}\mathbf{T}^{(k)} = \mathbf{M}_{pp} + (\mathbf{t}^{(k)})^{T}\mathbf{M}_{ps}^{T} + \mathbf{M}_{ps}\mathbf{t}^{(k)} \\ &\quad + (\mathbf{t}^{(k)})^{T}\mathbf{M}_{ss}\mathbf{t}^{(k)}\end{aligned} \tag{16}$$

Finally, $\mathbf{t}(\boldsymbol{\alpha})$ in Eq. (6) is calculated in the perturbed system using the IIRS technique [6] of Eq. (15). A guideline for deciding the number of iterations in the IIRS is given in Fig. 1.

IV. Numerical Examples

In this section, we examine the efficiency of the IIPM through numerical examples of damage detection. The first example is the flexural vibration of a cantilever beam which is investigated for the assessment of the selection of optimality and solution accuracy in damage detection [13]. The finite element model is described in Fig. 2a. The methods of selection of PDOFs are the SEM and the TLCS combined with a substructuring scheme, as shown in Figs. 2b and 2c, respectively.

The width (b) of the rectangular cross section was defined as the design variable. The widths of four elements were arbitrarily reduced as shown in Fig. 3a. For the inverse solutions of each selection technique, the SEM is applied in Fig. 3b and the TLCS is applied in Fig. 3c. The detailed solution values are presented in Table 1. Solutions of both selection methods exhibit similar convergence rates and accuracies, although the SEM needs much more computational time. This is the reason why we apply the TLCS, instead of the SEM, as the scheme of selection of PDOFs.

The next example is that of a cantilever plate. As shown in Fig. 4a, the total number of elements is 48, and the total number of nodes and DOFs are 65 and 390, respectively. The method for selecting PDOFs is TLCS, the same as the previous example. In Fig. 4b, the nodes marked with circles represent the positions of PDOFs, while perturbations are applied for the elements in colored boxes; these are the 9th and the 16th elements in which the amounts of perturbations are -25% and -20%.

Table 2 shows the results of eigenvalue analysis of the baseline system and the perturbed system. The magnitude of change between the baseline system and the perturbed system is under 5%. From the modal response of the perturbed system, the inverse problem is solved. In the case of IIPM, the total number of iterations for constructing the transformation matrix is only five.

Figure 5a shows the results from IPM which takes 18106 s for calculation. Through a comparison of Figs. 5a and 5b, it is observed that IIPM is much more accurate and efficient than IPM; the detailed results are given in Table 2. When IIPM is used, the required number of modes to get a reliable solution is only two whereas IPM requires seven modes and its calculation takes only 695 s. It should be mentioned that IIPM is applicable to the practical problems of damage detections or system identifications with reliability and efficiency whereas IPM cannot provide efficient applicability to the practical problems.

V. Conclusions

This Note presents an efficient methodology for identifying structural changes using a nonlinear iterative inverse perturbation method. Through implementation of the reduced system method, errors in the transformation matrix can be minimized. The method yields remarkable improvements in terms of solution accuracy and the use of computational resources. The numerical examples demonstrate the effectiveness of the proposed method in the flexural beam bending and the cantilever plate identification problems. For the same perturbed system, the proposed method needs far fewer modes compared with previous methods. The computational times and consumption of computer memory are also dramatically reduced. In spite of the small number of modes that are involved, the proposed method is both highly efficient and accurate.

Acknowledgment

This work was supported by the Korea Science and Engineering Foundation (KOSEF) through the National Research Laboratory Program funded by the Ministry of Science and Technology (No. R0A-2008-000-20109-0).

References

[1] Doebling, S. W., Farrar, C. R., Prime, M. B., and Shevitz, D. W., "Damage Identification and Health Monitoring of Structural and Mechanical Systems from Changes in Their Vibration Characteristics: A Literature Review," Los Alamos National Rept. LA-13070-MS, 1996.

[2] Choi, Y. J., "System Reduction and Selection of Degrees of Freedom in Structural Dynamic Inverse Problem," Ph.D. Dissertation, In-ha University, In-chon, Korea, 2001.

[3] Kim, K. O., Cho, J. Y., and Choi, Y. J., "Direct Approach in Inverse Problems for Dynamic System," *AIAA Journal*, Vol. 42, No. 8, 2004, pp. 1698–1704.
doi:10.2514/1.941

[4] Guyan, R. J., "Reduction of Stiffness and Mass Matrices," *AIAA Journal*, Vol. 3, No. 2, 1965, p. 380.
doi:10.2514/3.2874

[5] O'callahan, J., "A Procedure for an Improved Reduced System (IRS) Model," *Proceedings of 7th International Modal Analysis Conference*, Union College, Schenectady, NY, 1989, pp. 17–21.

[6] Friswell, M. I., Garvey, S. D., and Penny, J. E. T., "The Convergence of the Iterated IRS Method," *Journal of Sound and Vibration*, Vol. 211, No. 1, 1998, pp. 123–132.
doi:10.1006/jsvi.1997.1368

[7] Kim, K. O., and Kang, M. K., "Convergence Acceleration of Iterative Modal Reduction Methods," *AIAA Journal*, Vol. 39, No. 1, 2001,

pp. 134–140.
doi:10.2514/2.1281

[8] Kim, K. O., and Choi, D. H., "System Condensations for Inverse Problems of Linear Dynamic Structures," *Inverse Problems in Science in Engineering*, Vol. 14, No. 3, 2006, pp. 267–285.

[9] Henshell, R. D., and Ong, J. H., "Automatic Masters from Eigenvalues Economization," *Earthquake Engineering and Structural Dynamics*, Vol. 3, No. 4, 1974, pp. 375–383.
doi:10.1002/eqe.4290030408

[10] Cho, M., and Kim, H., "Two-Level Scheme for Selection of Degrees of Freedom by Energy Estimation Combined with Sequential Elimination," *International Council of the Aeronautical Sciences 2004 Congress*, International Council of the Aeronautical Sciences (ICAS), Yokohama, Japan, 2004, p. 8.

[11] Cho, M., and Kim, H., "Element-Based Node Selection Method for Reduction of Eigenvalue Problem," *AIAA Journal*, Vol. 42, No. 8, 2004, pp. 1677–1684.
doi:10.2514/1.5407

[12] Kim, H., and Cho, M., "Two-Level Scheme for Selection of Primary Degrees of Freedom and Semi-Analytic Sensitivity Based on the Reduced System," *Computer Methods in Applied Mechanics and Engineering*, Vol. 195, Nos. 33–36, 2006, pp. 4244–4268.
doi:10.1016/j.cma.2005.08.004

[13] Papadopoulos, M., and Garcia, E., "Sensor Placement Methodologies for Dynamic Testing," *AIAA Journal*, Vol. 36, No. 2, pp. 256–263.
doi:10.2514/2.7509

[14] Kim, H., and Cho, M., "Improvement of Reduction Method Combined with Sub-Domain Scheme in Large Scale Problem," *International Journal for Numerical Methods in Engineering*, Vol. 70, No. 2, 2007, pp. 206–251.
doi:10.1002/nme.1868

R. Ohayon
Associate Editor